ICANS XIX,
19th meeting on Collaboration of Advanced Neutron Sources
March 8 – 12, 2010
Grindelwald, Switzerland

DEVELOPMENT OF BUBBLE INJECTION TECHNIQUE IN JSNS MERCURY TARGET

Hiroyuki KOGAWA
Japan Atomic Energy Agency, 2-4 Shirakata-shirane
Tokai-mura, Ibaraki-ken 319-1195, Japan

and

Katsuhiro HAGA, Takashi NAOE, Hidetaka KINOSHITA,
Masato IDA, Masatoshi FUTAKAWA
Japan Atomic Energy Agency, 2-4 Shirakata-shirane
Tokai-mura, Ibaraki-ken 319-1195, Japan

ABSTRACT

A MW-class mercury target for the spallation neutron source will be subjected to the pressure waves induced by high-intense pulse-proton beam bombardment. The pressure waves load cyclic stress on a target vessel and degrade the vessel by pitting damage. Microbubbles injection into mercury is one of effective techniques to mitigate the pressure waves. We are carrying out development of bubble injection techniques from the viewpoint of the followings;

(1) development of microbubble generator to inject microbubbles in mercury
(2) investigation of bubble distribution in the mercury target and
(3) development of gas control system.

As for the microbubble generator, JAEA has succeeded to generate microbubbles in mercury by using swirl flow. The bubble distribution is investigated by using a target model filled with both mercury and water and by numerical simulations. Microbubbles could reach around a beam window under mercury flowing condition in the target. And the gas control test loop for bubbling is prepared to establish gas supply method and gas removal method from the flowing bubbly mercury.

1. Introduction

A mercury target is set at the Japanese Spallation Neutron Source (JSNS) of the Materials and Life science Facility (MLF) in the Japanese Proton Accelerator Research Complex (J-PARC). The mercury target is bombarded by a pulsed proton beam (Energy: 3 GeV, Repetition cycle: 25 Hz, Pulse duration: 1 μs, Final power in the project: 1 MW) to produce high intense neutrons for innovative sciences.

Pressure waves generated by the proton bombardment. The pressure waves propagate in mercury to a target vessel which is a container for activated mercury. The pressure waves shorten a lifetime of the target vessel not only by fatigue due to a cyclic load but also by the cavitation erosion, so-called pitting damage resulting from the pressure wave propagations [1]. Techniques on the pressure waves mitigation should be developed to realize the high power operation.

Injection of microbubbles with sufficient fraction into the mercury will mitigate the pressure waves [2] and the pitting damages on the target vessels [3]. To realize the

microbubbles injection into the mercury, bubbling system is being developed. The bubbling system consists of 2 parts. One is a bubbler to make the microbubbles into mercury. Another is a gas supplying system to the bubbler. They will be installed to the mercury circulation system which has been already operated in the MLF [4] during maintenance period in the summer 2011 based on power up schedule of the accelerator in J-PARC. Fig.1 shows a schematic drawing of the bubbling system. The bubbler will be set into a mercury target vessel and the gas supplying system will be set on the target trolley. The gas supplying system will have the apparatus to supply continuously gas to the bubbler with controlled flow rate.

A candidate bubbler is the swirl bubbler which is able to make small microbubbles in the lakes and the large tanks. However, the flow resistance will be high and swirl will remain in downstream from the bubbler which induces coalescence of microbubbles if it will be set in the pipe, such as the position where the bubbler is going to be installed in the mercury target.

The bubble distribution near the beam window is important to mitigate the pressure waves because the high pressure is generated there.

The mercury circulation system has high positioned pipes for a remote handling maintenance and heat exchanger (HEX) to remove the heat generated at the target. There is a possibility to occur a gas accumulation at those points, if the bubble can be removed at a surge tank by the buoyancy force. The gas accumulation in the pipe will induce the instability of the mercury flow, such as a decrease in flow rate and an increase in the flow resistance due to the reduction of the cross section area of the flow.

In this paper, a new concept swirl bubbler to reduce the flow resistance and to suppress the swirl at downstream from the bubbler will be described. The bubble distribution in mercury target and the gas accumulation behaviour will be discussed. The concerns found throughout experiments are introduced with future plant to be solved them.

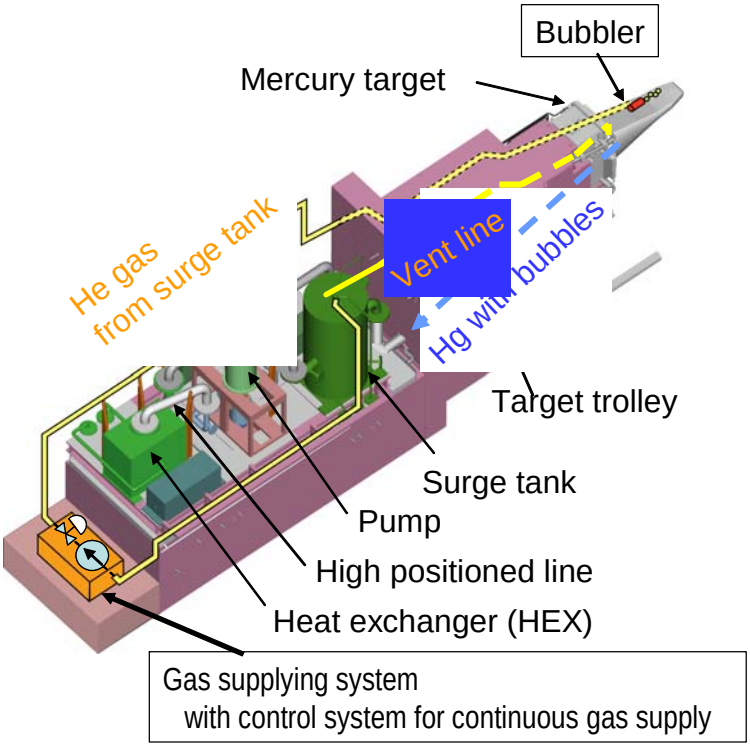

Figure 1 Schematic drawing with the mercury circulation system in JSNS

2. Invention of multi type swirl bubbler

2.1. Swirl type bubbler

Fig.2 (a) shows a shcematic drawing of a swirl bubbler. The swirl type of bubbler consists of a swirler and Venturi. The swirler is fastened guide vane to make the swirl flow in liquid. The venturi makes swirl velocity higher and makes pressure distribution at outlet of the venturi. Gas is injected from the center of the swirler to makes gas column at the center of the swirl bubbler. The gas column is bended at the outlet of the venturi by the Coanda effect. The bended column is broken down to the microbubbles due to the pressure distribution and the swirl velocity distribution at the outlet of the venturi.

The swirl bubbler has been applied for purifying the water in the pond, water tank etc. That is, the outlet of the bubbler facing to a stagnant wide area. On the other hand, since the bubbler will be installed into the mercury target, the outlet area will be limited. In this case, the swirl flow remains at the downstream from the bubbler and gathers the microbubbles at the center of the swirl to make the gas column again. To avoid the swirl at the outlet of the bubbler, a swirl stopper was installed at the downstream from the bubbler. The swirl stopper was effective to suppress the swirl at downstream from the bubbler, but the flow resistance (the pressure drop) increased.

The outer view of the swirl bubbler is cylindrical as shown in Fig.2. But the cross section of the mercury target where is going to be installed the bubbler is almost rectangular as shown in Fig.2. Therefore, the cross section for the flowing mercury is reduced in the bubbler and increase the pressure drop if a large single bubbler whose size much to the cross section of the target cross section is installed.

The reduction of the pressure drop in the bubbler and the suppression of the swirl at the downstream of the bubbler are concerns to install the bubbler into the real JSNS target .

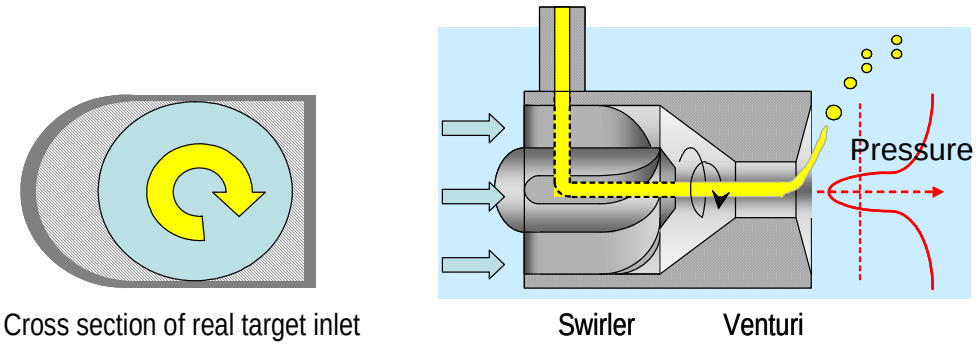

(a) Single type swirl bubbler

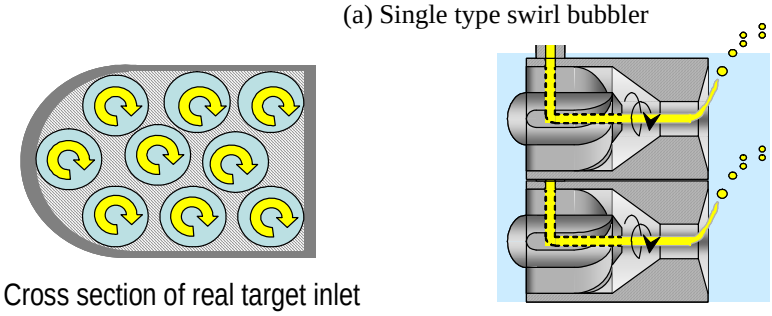

(b) Multi type swirl bubbler

Fig. 2. Schematic drawings of (a) single and (b) Multi type swirl bubblers

2.2. Multi type swirl bubbler

The cross section of the bubbler can be easily wider by arraying a lot of small bubbler as shown in Fig.2 (b). The length of the bubbler can be short by making the diameter small, which has a merit to reduce the pressure drop. Furthermore, arraying the bubbler parallel to the liquid flow causes an interference of the swirl at the outlet of the bubblers. Fig.3 shows bubble size distribution at the outlet of the single bubblers. Fig.3 shows the effect of the swirl stopper on the bubble sizes. The bubblers were installed to the same rectangular pipe under same liquid flow conditions. The generated bubbles from the single bubbler without the swirl stopper are larger than that from the single bubbler with the swirl stopper because of the swirl at the downstream from the bubbler. The bubble size became a few mm. The bubble sizes from the multi bubbler without the swirl stopper are as the same as those from the single bubbler with the swirl stopper.

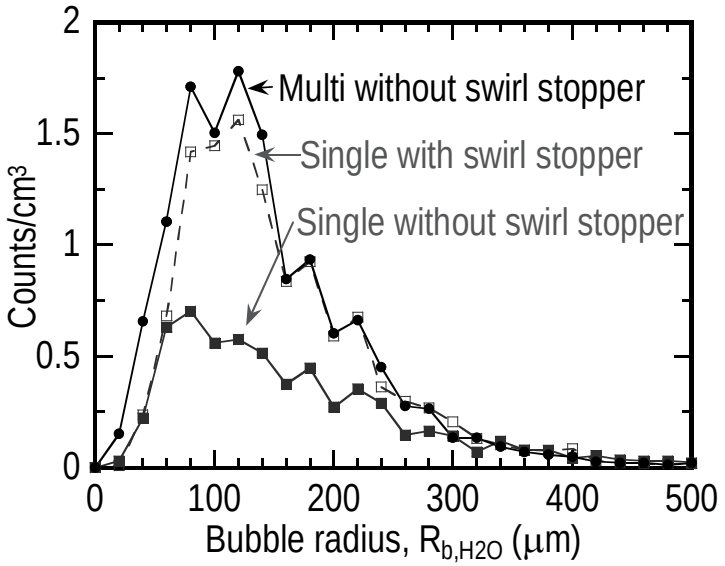

Fig. 3. Bubble size distribution at the downstream of each bubbler
(Tested in water of 5 L/s in flow rate and injected gas ratio to the water flow of 0.1%)

2.3. Pressure drop

Fig.4 shows the pressure drop divided by the liquid density against the flow velocity at the bubbler inlet, V_{in}, obtained by the following;

$$V_{in} = \frac{Q}{n \times \pi D^2/4} \quad (1)$$

where, n is the number of the bubbler, Q the flow rate of the liquid, D the inner diameter of the bubbler inlet as shown in Fig.2. The pressure drop of the multi bubbler without the swirl stopper reduced to 1/3 of that of the single bubbler with the swirl stopper while the generated bubble sizes are almost the same between them.

The pressure drop, ΔP, is expressed as following,

$$\frac{\Delta P}{\rho} = \frac{1}{2}(C_D + f)V_{in}^2 \quad (2)$$

where, ρ is the liquid density, C_D the pressure drop coefficient by the bubbler shape, *f* that by the friction between the liquid and the wall material. In Fig.4, the results of the pressure

drops in water and mercury are plotted. The pressure drops divided by the liquid densities of the same bubbler are the same independent of liquid. That is, the pressure drop by the friction in the swirl type bubbler is negligible low compared with that by the bubbler shape. The pressure drop in mercury can be estimated in water test.

The pressure drop in the bubbler should be less than 0.2 MPa in the real system. 14 Pa/(kg/m^3) of the pressure drop divided by the density corresponds with the 0.2 MPa of pressure drop in mercury. To install the real target, the velocity at the inlet should be less than 1.2 m/s. Since the operational flow rate of mercury in the real system is 41 m^3/h (683 L/min, 11.4 L/s), the inner diameter of the bubbler inlet should be more than 36.7 mm in the case that the 9 small bubblers are going to be arrayed.

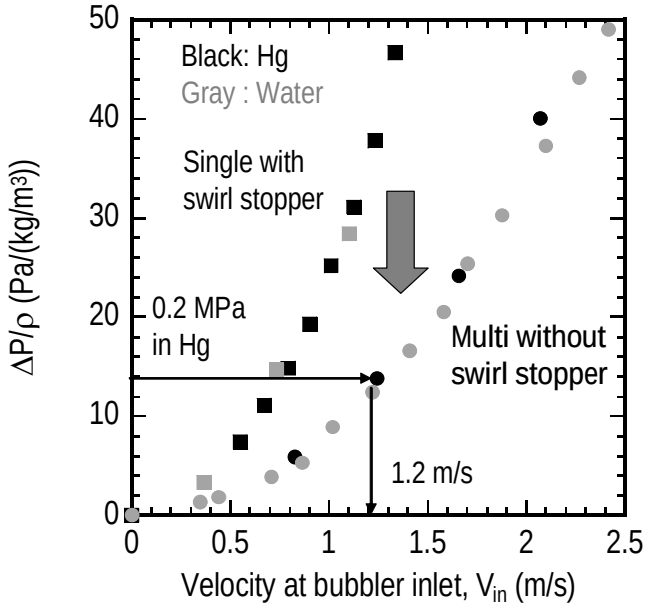

Fig. 4. Pressure drop in the bubbler against the flow velocity at bubbler inlet

3. Bubble distribution in JSNS target

3.1. Target model

Fig.5 shows the target model to investigate the bubble distribution of the target and pressure drop in the bubbler. The model size is 90 % smaller in horizontal and same size in height. The top wall of the model is made of acrylic resin to observe the microbubbles inside water and attached ones on the top wall. Other parts of the vessel are made of the stainless steel. The bubbler is set at the inlet of the model as shown in Fig.5. To distinguish the difference of the bubble distribution in water and mercury, the tests were carried out by utilizing the water loop in JAEA and TTF (the Target Test Facility) in ORNL (the Oak Ridge National Laboratory: U.S.A.). The flow rate was varied up to 27 m^3/h (7.5 L/s) in both tests.

3.2. Water test

The bubble distribution near the beam window is important to mitigate the pressure wave. A bubble distribution at the position A shown in Fig.5 are plotted in Fig.6. Fig.6 shows results in water in the case of the flow rate is 5 L/s. In Fig.6, the effect of the measured height, z, in the model is also shown. The frequency peak of the bubble size

appeared at 80 μm in radius independently of the height from the target bottom surface. The number of the bubbles increases with the height since the generated bubble rise up with water flow.

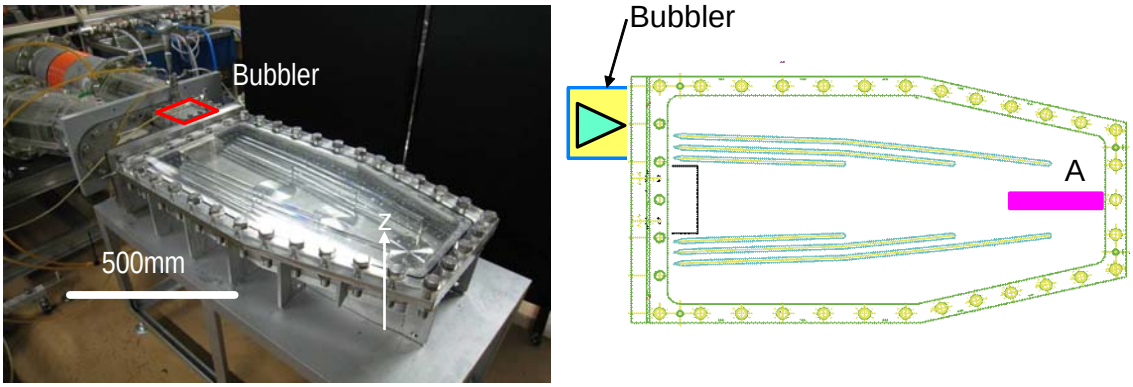

Fig. 5. JSNS mercury target model

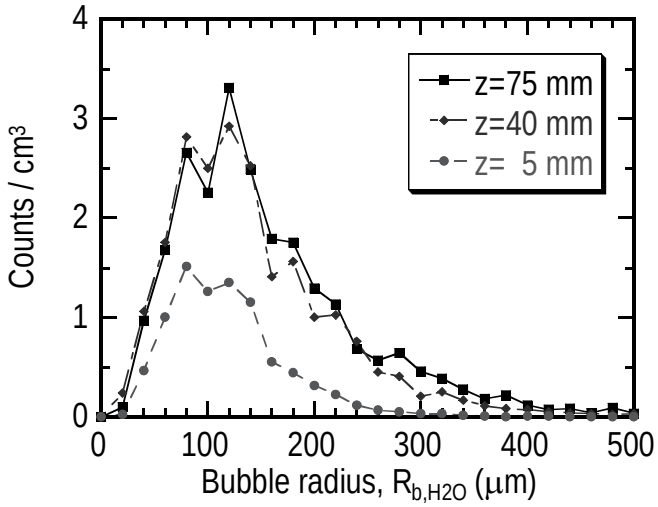

Fig. 6. Bubble distribution in water at position A shown in Fig. 5.
(Tested with multi bubbler without swirl stopper in water of 5 L/s in flow rate and injected gas ratio to the water flow of 0.1%)

3.3. Mercury test

Fig.7 shows the bubble size distribution in mercury at the position A in the case that the flow rate is 7.5 L/s. The bubbles are counted only that attached newly on the top wall. The peak appeared at 40 μm in bubble radius. For the pressure waves mitigation, not only the bubble size and also the bubble fraction is important which will be discussed in the next section.

Fig.8 shows the top view of the model in the case that the mercury flow rate was 5.5 L/s. A huge amount of the gas accumulated at the downstream from the flow guide vane, which was not observed in the water test. But the accumulating gas disappeared over the flow rate of 6.5 L/s. Since the operational flow rate is 11.4 L/s, this accumulating gas will not appear in the real system. However, we should carry out theoretical investigation on the mechanism to secure the no gas accumulation because temperature of the target vessel might increase due to low thermal conductivity of the gas compared with mercury.

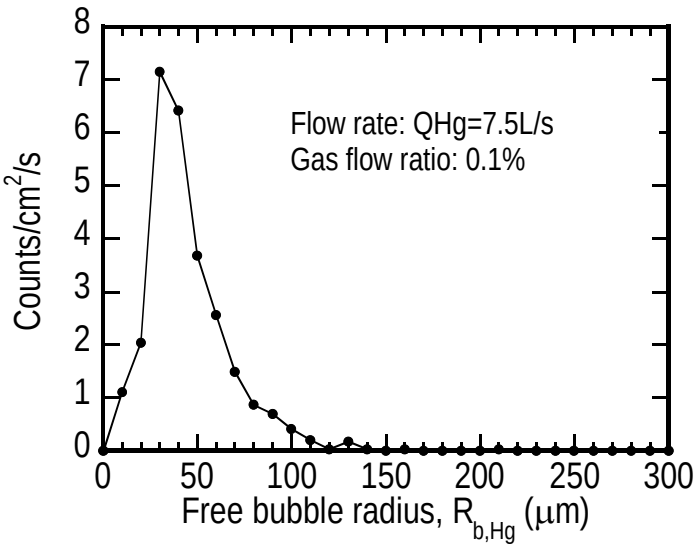

Fig. 7. Bubble size distribution in mercury by the multi bubbler without the swirl stopper

Fig. 8. Gas accumulation at the downstream of flow guide vane in the case of low mercury flow rate

3.4. Discussion

3.4.1. Bubble size

The bubble size in mercury became smaller than that in water comparing Fig.6. and Fig. 7. This is caused by not only the flow velocity of liquid but also the Weber number [5] which is the ratio of the inertia force on the bubble surface to the surface tension. The generated bubble radius, R_b, due to the turbulence between liquid and gas is proposed as the following equations [4],

$$R_b = 0.32\left(\frac{\sigma^3}{\rho^3\varepsilon^2}\right)^{1/5} \quad (3)$$

where, σ is the surface tension of liquid, ρ the density of the liquid and ε the visco-dissipation rate which depend only on the flow velocity and shape of the bubbler. Since the surface tension and the density of mercury are 7 times and 13 times larger than those of water, respectively, σ/ρ of mercury is smaller than those of water. The bubble size generated in mercury is smaller than that in water.

3.4.2. Estimation of bubble distribution in mercury and effect of pressure waves mitigation

By installing the multi bubbler into the target, the sufficiently small bubble size and low pressure drop will be achieved. However, the bubble fraction near the beam window is also important to mitigate the pressure waves in the mercury target.

Fig.9 shows the bubble fraction distribution in water height, which was obtained by the bubble volume in the image divided by the image volume (the image area multiplied by a focus depth of the camera; 10 mm). In this test, gas was injected with 0.1% to the water flow rate of 5 L/s. The bubble fraction increases with the measured height. That is easily imagined by the buoyancy force to the bubbles. The main bubble radius was 80 μm under the water flow condition of 5 L/s which corresponds to 0.5 m/s in flow velocity in the target. On the other hand, the main bubble radius is 40 μm under the condition that the mercury flow rate is 7.5 L/s which becomes 0.75 m/s in the target. The rising velocity of 80 μm radius bubble in water and 40 μm radius in mercury are 0.017 m/s and 0.020 m/s, respectively [6]. It is estimated that the bubble flows to 2.4 m and 3.0 m in horizontal direction for the bubble rising to 0.08 m (half height of the target) in 0.5 m/s flowing water and 0.7 m/s flowing mercury, respectively. The bubble fraction of the half height of the target is 0.025 % near the beam window in the 0.5 m/s flowing water as shown in Fig.9. In the 0.7 m/s flowing mercury, more bubbles will reach near the window. In the real target, since the flow velocity is c.a.1.0 m/s, much more bubbles reach near the window if the bubble radius keeps within 40 μm.

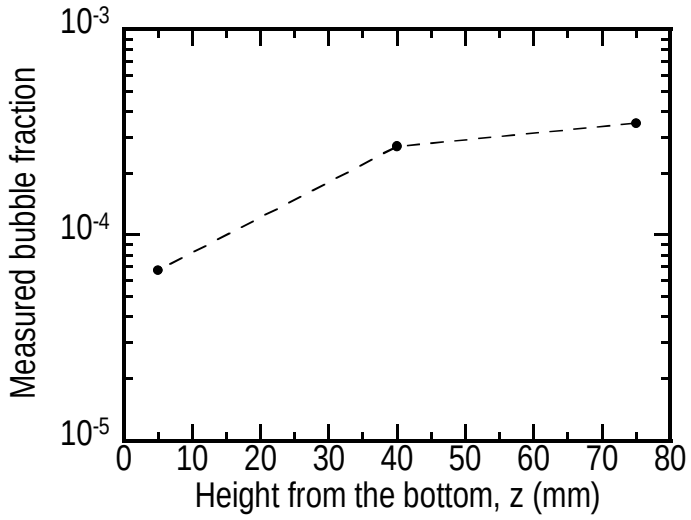

Fig. 9. Distribution of measured bubble fraction along height in water

A spark test in water by utilizing electrodes can provide a similar condition with mercury target. That is, high pressure amplitude of several ten MPa and high pressure rising time of a few micro seconds can be produced in water between the electrodes [7]. Pressure wave in water could be mitigated to 1/5 of that without bubbles by the microbubbles of 50 μm in radius and 0.025 % in bubble fraction. And bubbles effect in water and mercury are expected to the same by a numerical study [7]. We can expect such mitigation of the pressure waves in the real target.

4. Gas supplying system

4.1. Concept of gas supplying system

For the pressure waves mitigation, the bubbler should produce the microbubbles into mercury continuously. At moment, the gas to the bubbler is controlled by a mass flow controller from the pressure controlled buffer tank. The cover gas in the mercury surge tank is aspirated to the buffer tank through the compressor. The injected gas flows with mercury in the target to the surge tank. In the surge tank, the bubbles removed to the cover gas by the buoyancy force. In short, the bubbling system will consist of double closed loop of mercury and helium gas.

4.2. Mock up test with water loop

If the bubbles can not be removed in the surge tank, the bubbles will accumulate in the pipe and the heat exchanger (HEX) to induce the pressure drop increase in the mercury loop and/or choking of the mercury flow and decrease of the HEX ability.

It is important to verify the effect of the gas injection on the mercury flow. However, it is difficult to maintain mercury from the viewpoint of safety and its opaque characteristics. Therefore, the mock up test stand with water loop was constructed to (1) verify the gas accumulation behaviour and effect on the liquid flow and (2) point out the concerns which should be solved by the mercury loop. After that, the gas supplying mock up with a small mercury loop will be constructed to solve the concerns pointed out from the water test.

Fig.10 shows the schematic drawing of the gas supplying system test stand with water loop. Photographs of the main components are also shown in Fig.10. The pipes and components were designed with c.a. 1/2 size of the real mercury circulation system except a pump. A target model with vent line at the outlet of the target model was also installed in the loop at upstream of the surge tank like the real system. The test was carried out with same liquid flow velocity with the real system. The pipe, the surge tank, high positioned pipe and the inlet and outlet of the HEX were made of acrylic resin to observe the gas behaviour.

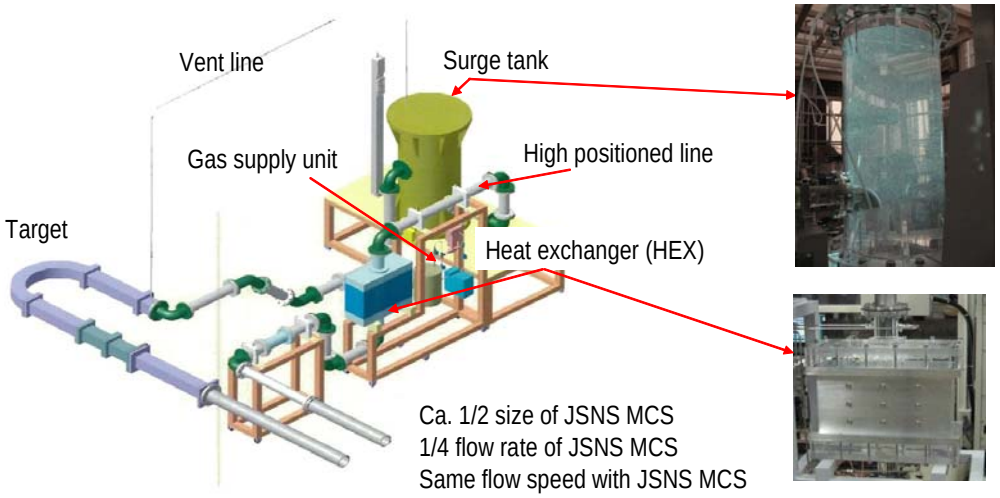

Fig. 10. Schematic drawing of water loop with gas supplying system

Fig.11 shows the gas accumulating behaviour at some points. Microbubbles were generated by the single swirl bubbler with the swirl stopper as shown in Fig.11 (a). Fig.11

(b) shows the behaviour at outlet of the target model. The microbubbles rising up on the top wall coalesce to large bubbles. The large bubbles flows with water and almost of those were vented from the vent line. The large bubbles not vented from the vent line flowed with water to the surge tank and those were removed to the cover gas by the buoyancy force. The microbubbles remain in the surge tank. The remained microbubbles were entrained by water at outlet of the surge tank and flowed with water without accumulation at the high positioned pipe. However, the gas accumulation was observed as a gas layer in the top of the HEX as shown in Fig.11(c). The height of the gas layer increased with the operational time. In the top of the HEX, the flow velocity of water decreased due to the wider cross section compared to the pipe and complicated flow pattern, such as a circulation flow induced by a jet flow hitting on a block of the heat exchanging region. Because of those effect, the microbubbles flowed into the HEX would be raised up on the top wall of the HEX to coalesce and would makes the gas layer.

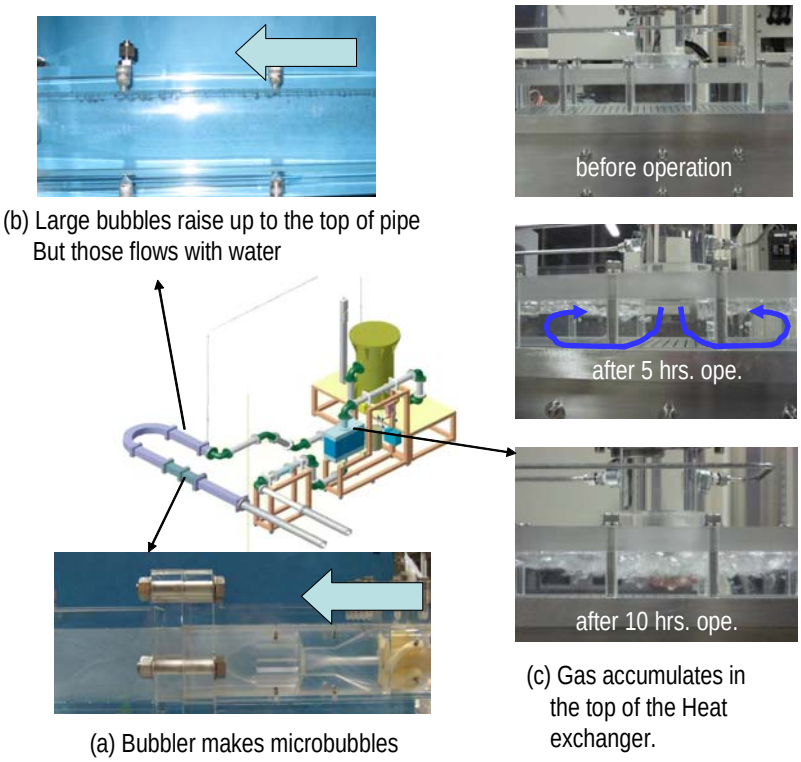

Fig. 11. Gas accumulation behaviour at (a) outlet of the bubbler, (b) outlet of the target model and (c) top of the heat exchanger

4.3. Discussion – Effect of the gas accumulation in the HEX on the liquid flow –

If the gas layer goes through the block of the heat exchanger region, the cooling ability of the HEX will be worse and the pressure drop will be high. It is important to concern whether the height of the gas layer saturate or not for the long and stable operation of the real system.

Fig.12 shows the time history of the gas layer height. It seems to saturate at c.a. 20 mm after 80 hours operation. The phenomenon was also observed that the water entrained the gas and the gas flowed with water as bubbles. The gas entrainment becomes easy to occur with decrease of the liquid height [8]. It is guessed that the entrained gas rate increases with decrease of the liquid height. The amount of entrained gas is considered to balance with that of flowing into the HEX when the gas layer height becomes c.a. 20 mm.

Fig.13 shows the histories of water flow rate and pump head. Time scale is same with that of in Fig.12. Even if the gas accumulation occurs, the flow rate of water and the pump head were stable.

The density, surface tension and viscosity are quite different between mercury and water. A numerical model to simulate the gas layer height in the HEX will be necessary to estimate and assess the real system. And small mercury loop is now being constructed to verify the numerical model in mercury.

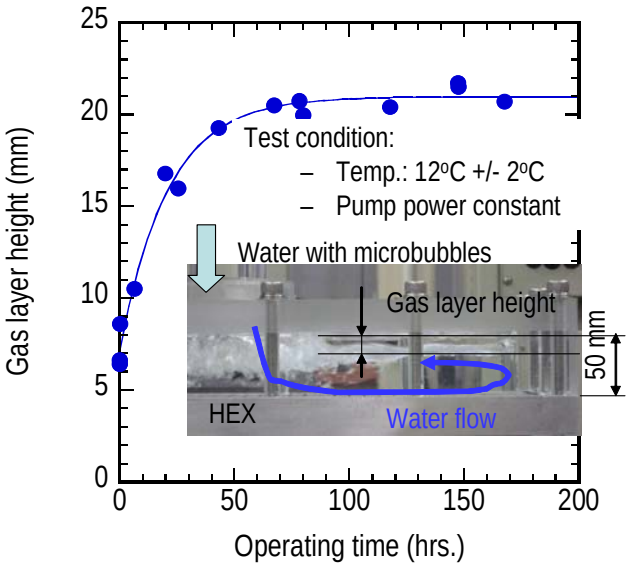

Fig.12. Time history of a gas layer height in the heat exchanger (HEX)

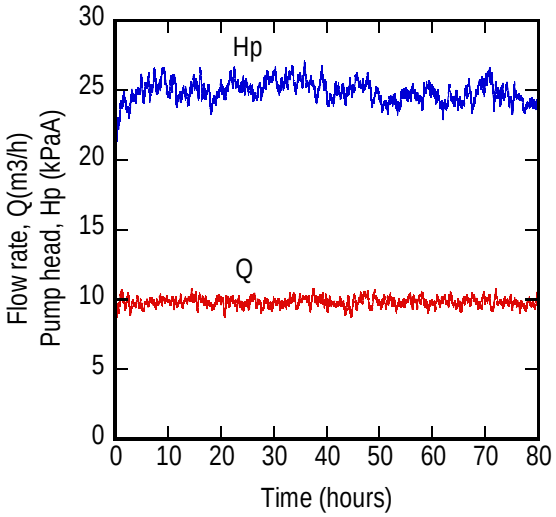

Fig. 13. Time histories of water flow rate and pump head while gas supplying to the bubbler and gas accumulating in the HEX

5. Summary

The development on the bubbling system is being carried out to install it during the maintenance period in the summer 2011. At moment, our knowledge and concerns are the followings;

- Multi swirl bubbler is effective on reduction of pressure drop and suppression of the swirl at downstream of the bubbler. To make the pressure drop less than 0.2 MPa the inlet velocity to the bubbler should be designed less than 1.2 m/s.

- The microbubbles can reach near the beam window, which will reduce the pressure wave to 1/5 of the no-bubble condition at least.
- It was predicted from water test that the gas accumulation does not so harmful to control constant gas formation.
- The gas accumulation in the HEX will be saturated. But the amount has not been estimated yet. Numerical study and experiment in mercury will be carried out to estimate the behavior in the real system.

Acknowledgement

We thank to Prof. Harumichi Kyotoh in Tsukuba University for the recommendation of designing the bubbler.

We also appreciate to Mr. Bernei Riemer, Mr. Mark Wendel and Mr. David Felde in the Oak Ridge National Laboratory for kindly help to carry out the bubbler tests in mercury.

Reference

1. M.Futakawa, et. al., *J. Nucl. Sci. and Tech.* **40** (2003) 895.
2. K.Okita, et. al., *J. Fluid Sci. and Tech.* **3** (2008) 116.
3. T.Naoe, et. al., *Nucl. Inst. & Meth. in Phys. Res. A* **586** (2008) 382.
4. H.Kogawa, et. al., *Nucl. Inst. & Meth. in Phys. Res. A* **600** (2009) 97.
5. C.Garrett, et. al., *J. Phy. Oceanograpy* **30** (2000) 2163.
6. F.N. Peebles, H.J. Garber, *Chem. Engng. Progr*. **49** (1953) 88.
7. M.Ida, et. al., *in this proceedings.*
8. H.Madarame, et. al., *Nucl. Eng. And Design*. **120** (1990) 193.